# Results of the Spectral Diagnostics of a Low-current Vacuum Arc with Cu cathode[1]

S.A. Chaikovsky, M.B. Bochkarev,* I.V. Uimanov*

*Institute of High Current Electronics, Akademichesky Ave, 2/3, Tomsk, 634055, Russia, 3822-49-21-33, 3822-49-77-16, stas@ovpe.hcei.tsc.ru*
*Lebedev Physical Institute, Leninsky Ave, 53, Moscow, 119991, Russia, 495-132-64-70, 495-132-68-07, stas-ch@sci.lebedev.ru*
**Institute of Electrophysics,Amundsena str, 106, Ekaterinburg, 620016, 343-267-87-68, maxim@iep.uran.ru, uimanov@iep.uran.ru*

**Abstract – Due to extremely low intensity of a self-radiation of the very low-current (1-10 A) vacuum arcs a detail research of their properties requires a high sensitivity along with a high spectral, spatial or temporal resolution of diagnostic device. The paper presents some experimental results on the spectral and spatial features of the low-current arc. Our experiments confirm that a visible line spectrum of the vacuum arc is hardly reflects the parameters of the densest and hottest regions of the cathode spot, giving mainly the information about the lower density surrounding plasma.**

## 1. Introduction

Explosive electron emission plays decisive role in vacuum discharges. Micro explosion on the cathode surface typically takes place during $10^{-10}$-$10^{-8}$ s and results in dense (over $10^{20}$ cm$^{-3}$) plasma production with the typical spatial dimension of few microns [1]. An unique object for experimental study of the vacuum discharges is a low-current vacuum arc with the current level of 1-10 A. In this case a cathode spot consists from only one emission centre. Such features of the vacuum arcs as burning instabilities and cycling, high-frequency fluctuations of the burning voltage and current, spontaneous extinction become the most prominent. However, due to extremely low intensity of a self-radiation of the low-current arcs a detail research of their properties requires a high sensitivity along with a high spectral, spatial or temporal resolution of diagnostic device. This is one of the reasons that the observations of cathode spot were performed mainly at currents of several tens amperes.

In Institute of Electrophysics, Ural Branch of RAS experimental researches of such low-current arcs are performed. The behavior of the emission centre plasma was before investigated using electric probes, high-speed streak camera and photomultiplier (see, for example, [2]). One of the purposes of these works was an attempt to find out the correlations between the noise-like fluctuations of the burning voltage, the light emission intensity and the emission centers recycling processes. It seems to be useful apply also spectroscopic measurements in these researches to give deeper insight into the very low-current cathode spot functioning.

This paper is aimed on the investigation of the spectral and spatial properties of the visible radiation of the explosive emission centers in the low-current vacuum arc. Namely, visible spectra of the vacuum arc were collected without temporal resolution, the spectral lines were identified, dependencies of the radiation intensity and plasma parameters on the arc current were obtained, attempt to register a spectrum with the spatial resolution was performed. Thus, the paper presents some experimental results on the spectral features of the low-current arc. We believe that the results will be useful for interpretation of the processes in the emission centers and make it wider the existing experimental database on the cathode spot plasma properties.

## 2. Experimental setup

The experiments were carried on with the vacuum arc at the current level of 3-30 A. Arc current was adjusted by the charge voltage of the pulse generator based on a 75 Ohm cable. The current pulse length was equal to 700 ns. The cathode was made of high purity copper and cleaned by preliminary arcing in vacuum and had a diameter of 150 μm. The anode was made of tungsten wire. The anode-cathode gap was of 150 μm. The arc was triggered with a thin tungsten pin powered by 20-ns high voltage pulse. Experiments were carried on at the basic vacuum < $10^{-8}$ Torr. The vacuum arc was initiated on the lateral side of the cathode, so the cathode spot could be viewed by a spectrograph as a whole. Diagnostics included high-frequency current and voltage probes, spectrograph MS-257 with a sensitive CCD matrix. An input slit of

[1] The work was supported by Program of the fundamental researches of the Presidium RAS “Fundamental problems of the nano- and picosecond high power electronics” and in part by RFBR grants # 05-02-08240-ofi_a and # 05-02-17612.

the spectrograph was illuminated with help of either glass objective, or a quartz lens. The spectrograph had the input focal length of 220 mm and an aperture ratio of ¼, so the projection objective was chosen to match approximately this value. With a grating of 2400 g/mm and slit width of 100 μm the spectrograph provided dispersion of 0.037 nm/px (1.4 nm/mm) and spectral resolution of 0.3 nm.

### 3. Spectral lines identification

In order to find out the spectral distribution of the line radiation the spectra were collected with the grating of 2400 g/mm with the resolution of 0.3 nm/mm in the spectral ranges 197-239, 212-255, 302-343, 401-442, 492-530, 611-644 nm.

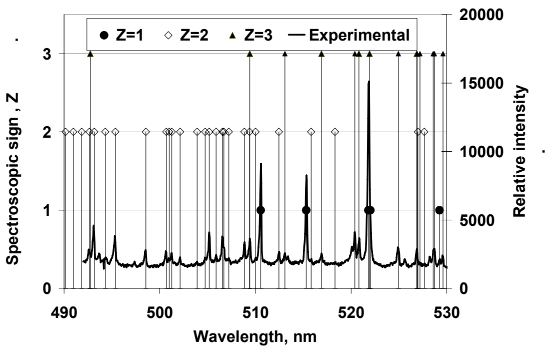


Fig.1. Experimental spectrum in the range 490-530 nm and positions of the spectral lines identified.

Figure 1 present the experimental spectrum obtained at the arc current of 15 A in the wavelength range of 490-530 nm together with the positions of the most persistent lines of the copper ions with in the different ionization stages. The spectroscopic sign is an ion charge plus 1, i.e. the neutral atom has a spectroscopic sign of 1. It should be noted that the spectral features had no significantly dependence on the arc current, so the line identification was performed at higher level of the current. In order to enlarge the intensity of the spectra and raise over the noise level the spectra were detected by accumulation of 20 shots of the arc.

Table 1. Spectral lines identified.

| λ, nm | Z | Log $(gf)_1$ | $E_1$, Ev | $Term_1$ | Log $(gf)_2$ | $E_2$, Ev | $Term_2$ |
|---|---|---|---|---|---|---|---|
| 197.9956 | 2 | -0.52 | 2.831 | 4s 3D | -0.177 | 9.091 | 4p3D* |
| 198.9855 | 2 | -0.78 | 2.831 | 4s 3D | -0.751 | 9.059 | 4p3D* |
| 199.9697 | 2 | -0.03 | 2.718 | 4s 3D | -0.104 | 8.913 | 4p3D* |
| 203.5854 | 2 | -0.13 | 2.974 | 4s 3D | -0.086 | 9.059 | 4p3D* |
| 203.7127 | 2 | -0.22 | 2.831 | 4s 3D | -3.649 | 8.913 | 4p3D* |
| 204.3802 | 2 | -0.07 | 2.718 | 4s 3D | 1.71 | 8.779 | 4p1F* |
| 205.498 | 2 | -0.26 | 2.831 | 4s 3D | -0.495 | 8.860 | 4p1D* |
| 207.8663 | 2 | 0.122 | 8.231 | 4p 3P* | 0.122 | 14.191 | 4d 3S |
| 209.8398 | 2 | 0.185 | 8.518 | 4p 3F* | 0.185 | 14.422 | 4d 3F |
| 210.4797 | 2 | -0.49 | 2.974 | 4s 3D | -0.586 | 8.860 | 4p1D* |
| 211.21 | 2 | -0.09 | 3.255 | 4s 1D | -0.031 | 9.121 | 4p1P* |
| 211.731 | 2 | 0.656 | 8.483 | 4p 3F* | 0.656 | 14.334 | 4d 3G |
| 212.298 | 2 | -0.07 | 3.255 | 4s 1D | -0.238 | 9.091 | 4p 3D* |
| 212.6044 | 2 | -0.26 | 2.831 | 4s 3D | -0.252 | 8.659 | 4p 3F* |
| 213.4341 | 2 | 0.779 | 8.518 | 4p 3F* | 0.779 | 14.322 | 4d 3G |
| 213.5981 | 2 | 0.41 | 2.718 | 4s 3D | 0.459 | 8.518 | 4p 3F* |
| 214.8984 | 2 | -0.51 | 2.718 | 4s 3D | -0.431 | 8.483 | 4p 3F* |
| 216.132 | 2 | -1.73 | 8.860 | 4p1D* | -1.73 | 14.592 | 4d 3G |
| 217.4982 | 2 | 0.234 | 8.913 | 4p3D* | 0.234 | 14.609 | 4d 1G |
| 218.963 | 2 | -0.26 | 3.255 | 4s 1D | 0.15 | 8.913 | 4p 3D* |
| 219.2268 | 2 | 0.15 | 2.831 | 4s 3D | 0.217 | 8.483 | 4p 3F* |
| 219.5683 | 2 | -.038 | 8.779 | 4p 1F* | -0.038 | 14.422 | 4d 3F |
| 220.98 | 2 | 0.091 | 8.779 | 4p 1F* | 0.091 | 14.386 | 4d 3D |
| 221.0268 | 2 | -.003 | 3.255 | 4s 1D | -0.003 | 8.860 | 4p 1D* |
| 221.81 | 2 | -0.17 | 2.831 | 4s 3D | -0.122 | 8.417 | 4p 3P* |
| 222.8868 | 2 | -0.56 | 2.974 | 4s 3D | -0.514 | 8.533 | 4p 3P* |
| 224.2618 | 2 | 0.06 | 3.255 | 4s 1D | -0.249 | 8.779 | 4p 1F* |
| 224.7002 | 2 | 0.1 | 2.718 | 4s 3D | 0.147 | 8.231 | 4p 3P* |
| 227.6258 | 2 | -0.9 | 2.974 | 4s 3D | -0.853 | 8.417 | 4p 3P* |
| 228.6645 | 2 | -.538 | 8.913 | 4p3D* | -0.538 | 14.331 | 4d 3P |
| 236.989 | 2 | -0.67 | 3.255 | 4s 1D | -0.8 | 8.483 | 4p 3F* |
| 240.333 | 2 | -0.2 | 8.231 | 4p 3P* | -0.141 | 13.386 | 5s (31) |
| 241.234 | 3 | -1.73 | 9.967 | a4P | -1.729 | 15.103 | z4D* |
| 246.841 | 3 | | 24.046 | 3F4d2H | | 29.065 | 3F4f4<7>* |
| 254.4805 | 2 | 0.12 | 8.518 | 4p 3F* | -0.13 | 13.386 | 5s (31) |
| 324.754 | 1 | -.064 | | 4s 2S | -0.057 | 3.815 | 4p 2P* |
| 327.396 | 1 | -.369 | | 4s 2S | -0.367 | 3.784 | 4p 2P* |
| 402.7026 | 1 | -1.42 | 5.722 | | -1.42 | 8.799 | 4d' 4S |
| 403.2647 | 2 | -2.04 | 14.883 | 5p 3P* | -2.043 | 17.955 | 7s (31) |
| 405.678 | 1 | | 3.815 | 4p 2P* | | 6.869 | 4f 2F* |
| 421.6912 | 2 | -1.818 | 15.227 | 5p 1P* | -1.818 | 18.165 | 6d 3D |
| 427.5107 | 1 | -0.12 | 4.836 | 4p'4P* | -0.12 | 7.734 | 5s' 4D |
| 439.7 | 1 | | 5.503 | 4p'4D* | | 8.321 | 5s'' 2D |
| 438.642 | 3 | | | | | | |
| 435.197 | 3 | | | | | | |
| 435.28 | 3 | | | | | | |
| 435.524 | 3 | | | | | | |
| 437.14 | 3 | | | | | | |
| 437.343 | 3 | | | | | | |
| 437.7111 | 3 | | | | | | |
| 492.6424 | 2 | 0.08 | 14.334 | 4d 3P | 0.071 | 16.849 | 4f3<1>* |
| 493.1697 | 2 | 0.9 | 14.334 | 4d 3G | 0.915 | 16.846 | 4f3<6>* |
| 493.1554 | 2 | 0.3 | 14.331 | 4d 3P | 0.264 | 16.843 | 4f3<2>* |
| 494.3025 | 2 | -0.17 | 14.331 | 4d 3P | -0.2 | 16.837 | 4f3<2>* |
| 495.3724 | 2 | 0.91 | 14.609 | 4d 1G | 0.918 | 17.110 | 4f2<5>* |
| 497.4155 | 2 | -0.419 | 14.644 | 4d 1D | -0.419 | 17.135 | 4f 2<4>* |
| 498.5505 | 2 | 0.64 | 14.386 | 4d 3D | -0.255 | 16.871 | 4f 3<5>* |
| 500.6801 | 2 | 0.53 | 14.644 | 4d 1D | 0.576 | 17.118 | 4f 2<3>* |
| 500.9851 | 2 | 0.374 | 14.386 | 4d 3D | 0.374 | 16.859 | 4f 3<4>* |
| 501.262 | 2 | 0.73 | 14.416 | 4d 3F | 0.023 | 16.888 | 4f 3<4>* |
| 502.1279 | 2 | -0.738 | 14.386 | 4d 3D | -0.738 | 16.853 | 4f 3<3>* |
| 503.9016 | 2 | -0.02 | 14.644 | 4d 1D | -0.042 | 17.103 | 4f 2<2>* |
| 504.7348 | 2 | 0.632 | 14.416 | 4d 3F | 0.632 | 16.871 | 4f 3<5>* |
| 505.1793 | 2 | 0.85 | 14.422 | 4d 3F | 0.827 | 16.874 | 4f 3<5>* |
| 505.891 | 2 | 0.38 | 14.422 | 4d 3F | -0.366 | 16.871 | 4f 3<5>* |
| 506.5459 | 2 | 0.77 | 14.684 | 4d 1F | 0.764 | 17.129 | 4f 2<4>* |
| 506.7094 | 2 | 0.54 | 14.690 | 4d 3F | 0.6 | 17.135 | 4f 2<4>* |
| 507.2302 | 2 | -1.652 | 14.416 | 4d 3F | -1.652 | 16.859 | 4f 3<4>* |
| 508.8277 | 2 | -0.457 | 14.424 | 4d 3D | -0.457 | 16.859 | 4f 3<4>* |
| 509.379 | 2 | | | | | | |
| 510.0067 | 2 | 0.488 | 14.424 | 4d 3D | 0.488 | 16.853 | 4f 3<3>* |

| | | | | | | | |
|---|---|---|---|---|---|---|---|
| 510.554 | 1 | -1.51 | 1.388 | 4s2 2D | -1.6 | 3.815 | 4p 2P* |
| 512.4476 | 2 | -0.772 | 14.424 | 4d 3D | -0.772 | 16.843 | 4f 3<2>* |
| 513.1 | 3 | | | | | 14.4? | |
| 515.324 | 1 | -0.02 | 3.784 | 4p 2P* | 0.04 | 6.188 | 4d 2D |
| 516.897 | 3 | | | | | | |
| 520.087 | 1 | -0.77 | 5.419 | 4p' 2F* | -0.77 | 7.801 | 5s' 4D |
| 520.4 | 3 | | | | | 26.6 | |
| 520.834 | 3 | | | | | | |
| 521.82 | 1 | 0.26 | 3.815 | 4p 2P* | -0.3 | 6.189 | 4d 2D |
| 524.94 | 3 | | | | | 26.2 | |
| 525.052 | 1 | -0.74 | 5.520 | 4p'4D* | -0.74 | 7.880 | 5s' 4D |
| 526.9 | 3 | | | | | 26.7 | |
| 526.999 | 2 | | 8.231 | 4p 3P* | | 10.582 | 4s2 1D |
| 527.2 | 3 | | | | | 26.4 | |
| 528.353 | 1 | | 7.021 | 4p"2D * | | 9.366 | 4d" 2F |
| 528.2 | | | | | | 28.4 | |
| 528.6 | 3 | | | | | 26.6 | |
| 528.7 | 3 | | | | | 26.4 | |
| 529.252 | 1 | -0.44 | 5.393 | 4p'4D* | -0.44 | 7.734 | 5s' 4D |
| 529.6 | 3 | | | | | 26.4 | |
| 611.4493 | 2 | | 14.956 | 5p 1F* | | 16.983 | 5d 3F |
| 612.773 | 2 | | 6.789 | 6p 2P* | | 8.811 | 4d' 2D |
| 615.0384 | 2 | 0.229 | 14.969 | 5p 3F* | 0.229 | 16.984 | 5d 3F |
| 615.4222 | 2 | 0.17 | 14.883 | 5p 3P* | 0.17 | 16.896 | 5d 3S |
| 617.2203 | 2 | -2.009 | 14.980 | 5p 1D* | -2.009 | 16.987 | 5d 3D |
| 618.6884 | 2 | -1.4 | 14.980 | 5p 1D* | -1.4 | 16.983 | 5d 3F |
| 618.8676 | 2 | -0.032 | 14.985 | 5p 3P* | -0.032 | 16.987 | 5d 3D |
| 619.8092 | 2 | -0.478 | 14.969 | 5p 3F* | -0.478 | 16.968 | 5d 3D |
| 620.4261 | 2 | 0.085 | 15.227 | 5p 1P* | 0.085 | 17.224 | 5d 1D |
| 620.8457 | 2 | 0.043 | 15.245 | | 0.043 | 17.241 | 5d 1F |
| 621.6939 | 2 | | 14.956 | 5p 1F* | | 16.949 | 5d 3G |
| 621.9844 | 2 | 0.543 | 15.212 | 5p 3F* | 0.543 | 17.204 | 5d 3G |
| 623.379 | 1 | | 6.944 | 4p" F* | | 8.931 | 4d' 4D |
| 626.1848 | 2 | 0.058 | 15.005 | 3Fsp1F* | 0.058 | 16.984 | 5d 3F |
| 627.3349 | 2 | 0.805 | 14.969 | 5p 3F* | 0.805 | 16.944 | 5d 3G |
| 630.1004 | 2 | 0.702 | 15.245 | | 0.702 | 17.212 | 5d 1G |
| 631.2491 | 2 | 0.159 | 15.281 | 5p 3D* | 0.159 | 17.244 | 5d 3F |
| 637.784 | 2 | -0.412 | 15.005 | 3Fsp1F* | -0.412 | 16.948 | 5d 3P |
| 640.3384 | 2 | -0.17 | 15.171 | 4d 1S | -0.32 | 17.106 | 4f 2<2>* |
| 643.2416 | 2 | | 16.843 | 4f3<2>* | -0.177 | 18.769 | 6g 3<3> |

The Table 1 presents the list of the lines observed. Also included are: decimal logarithms of product of the oscillator strength *f* and the statistical weight *g*, level energies *E* and terms of the lower and upper states. The lines wavelengths and other data were taken mainly from [3] and only few data were from [4, 5, 6, 7].

These data analysis shows that the most prominent are the CuI atomic lines with the excitation energies $E_{ex}$ = 3.78-8.9 eV, clearly observed a lot of lines belonging to CuII ions with $E_{ex}$ = 8.23-18.2 eV. Very weak are the lines of the CuIII ions with $E_{ex}$ up to 33.9 eV. The most bright lines in the spectra have the excitation energy from 3.8 to 16.9 eV. No lines of tungsten (anode material) were detected.

## 4. Spectral intensity dependence on the arc current and the plasma parameters

When the arc current was varied there were no significant changes observed in the spectra. The dependence of the total radiated energy in a few spectral ranges (i.e. integral under spectral profile) on the arc current is approximately linear. At the currents $I \approx$ 3-7 A the dependence seems to be absent, but more experimental statistics is required to state this fact with confidence.

From the whole spectral lines set a few pairs of lines were chosen for estimates of plasma parameters. Despite of the measurements are temporal and space integrated we, nevertheless, ventured to infer the electron temperature $T_e$ and the electron density $N_e$ using LTE approximation. The electron temperature values produced from the ratio of (CuI 521.8 nm/CuI 510.554 nm) lines were ≈ 0.7 eV at the arc currents 3-30 A. It is interesting to note that the line ratio of (CuI 521.8 /CuI 510.554) was approximately equal to ratio of their $f{\cdot}g$ values, that could be a confirmation of the plasma optical transparency. The electron temperature values inferred from the line ratios (CuII 212.299/CuII 212.600) and (CuII 211.21/CuII 211.731) were obtained to be ≈ 1.6-1.8 eV and did not depend clearly on the arc current. The reason of the low accuracy is overlapping of these lines with other bright lines. More reliable seems to be measurements using (CuII 224.26/CuII 224.7) line ratio. The spectra in vicinity of these lines are shown in Figure 2 for various value of the arc current. Table 2 shows the results of the estimates.

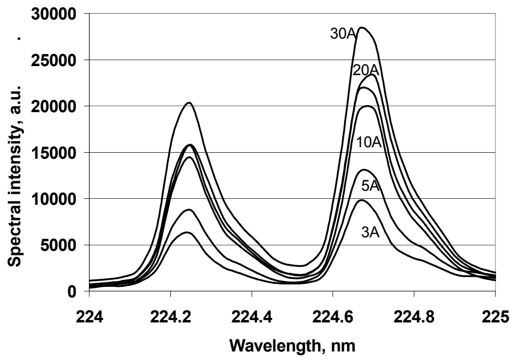


Fig.2. Spectra in the region of CuII 224.26 nm and CuII 224.7 nm lines at the arc currents *I* = 3, 5, 10, 15, 20 and 30 A.

Table 2. Electron temperature and electron density.

| *I*, A | 3 | 5 | 10 | 15 | 20 | 30 |
|---|---|---|---|---|---|---|
| $T_e$, eV | 1.24 ±5% | 1.22 ±7% | 1.5 ±6% | 1.58 ±14% | 1.54 ±14% | 1.65 ±14% |
| $N_e$, $cm^{-3}$ | - | 5.2 $x10^{17}$ | 2.9 $x10^{17}$ | 4 $x10^{17}$ | 8.4 $x10^{17}$ | 23.5 $x10^{17}$ |

The relative intensities of the CuI and Cu II lines were observed to be more sensitive to the arc current value. This is demonstrated by figure 3, where the CuI 510.5 nm и CuII 509.3 nm lines are shown. A line intensity ratio for ions with different ionization states depends not only electron temperature, but an electron density also [8]. This allows roughly estimate value of the electron density having an independently measured electron temperature. Values of the electron density evaluated are presented in the Table 2.

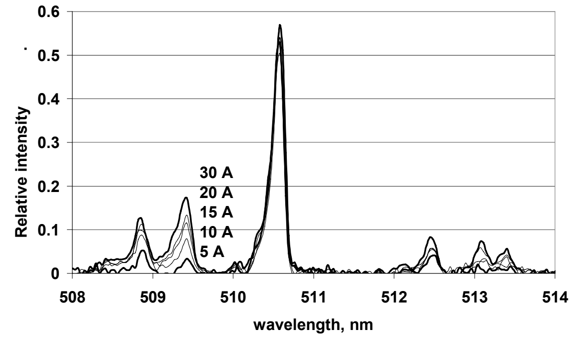


Fig.3. Spectra in the region 508-514 nm. The intensity of the CuII 509.3 line permanently increases along with the arc current.

## 5. Spatial resolved spectral measurements

In the experiments the spectrum with a spatial resolution of 30 mkm at the current of 30 A was registered. The spectrum was obtained in single arc shot in order to prevent possible displacement of the cathode spot from one shot to others. This spectrum is shown in Figure 4. Numerical analysis of the spectrum showed that dimension of the regions where spectral lines radiate is approximately two times larger then the region where continuum radiation dominates. Figure 5 shows spatial distribution of the intensity in the band of 0.4 nm around the line CuI 521.8 nm and around wavelength 523.65 nm, where no obvious lines were registered. The FWHM of the radiation spatial profile is of 50 μm for the continuum radiation and of 100 μm for the line radiation.

## 6. Short discussion and conclusion

On the whole the results of the experiments performed at the low arc current are in agreement with the previous data at the higher current level. The most prominent lines in spectra were also observed in [5, 6]. The high luminosity region size (order 100 μm) in the light of the atomic lines can be explained either transient excitation/radiation processes which typical times ($1/A \approx 10$ ns) are comparable with the life time of a small emission center (~ 10 ns), following expanding and cooling of its plasma or rapid movement of these small centers [9]. The first reason seems to be more reliable, because low electron density and low electron temperature could not be attributed to dense non-ideal plasma of the emission centers. In any case, despite of rich spectrum of the arc in visible and UV region, this portion of the spectrum does not related to the most dense and hot plasma of the cathode spot. In order to develop a diagnostic based on self-radiation of the cathode spot a step into the VUV and EUV spectral ranges seems to be useful.

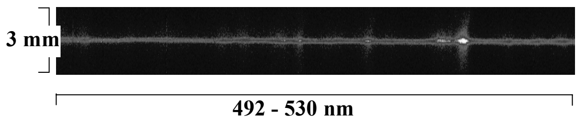


Fig.4. Spectrum with spatial resolution

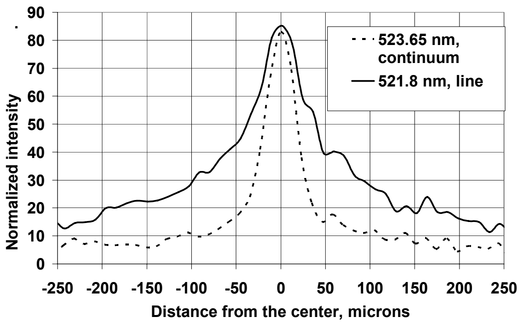


Fig.5. Spatial distributions of the line and continuum radiation

## References


[1] G.A.Mesyats, *Ectons in vacuum discharge: breakdown, spark, arc*, Moscow, Science, 2000, 424 p.

[2] M. Bochkarev, *in Proc. 21st International Symposium on Discharges and Electrical Insulation in Vacuum,* 2004, pp.241-244.

[3] Интернет-ресурс: *AMODS (Atomic Molecular and Optical Database Systems). http://amods.kaeri.re.kr*

[4] A.N. Zaidel // Tablitsy spectral'nyh linii. Moscow, Gostehteorizdat, 1952, 560 s.

[5] H. Rosenthal, I. Beilis, S. Goldsmith and R.L. Boxman// J. Phys. D: Appl. Phys. **29**, 1245 (1996).

[6] A.Anders and S.Anders// J.Phys.D: Appl.Phys. **24**, 1986 (1991).

[7] Интернет-ресурс: *A NIST Atomic Spectra Database. http://physics.nist.gov*

[8] H.R.Griem, *Plasma spectroscopy,* Moscow, Atomizdat, 1969, 451 p.

[9] S.Anders, A.Anders and B. Juttner// J.Phys.D: Appl.Phys. **25**, 1591 (1992).